Volume : 4 | Issue : 3 | March 2015 • ISSN No 2277 - 8179

Research Paper

Chemistry

KEYWORDS : SBT-SBN ceramics, dielectric and ferroelectric properties, XRD, Raman characterization

Dielectric properties of novel $Sr_{0.3}Ba_{0.7}Ti_{O3}$-$Sr_{0.3}Ba_{0.7}Nb_2O_6$ composite ceramic

Abhilash Kumar	Department of Physics, Amity University, Gurgaon, Haryana, INDIA
Manisha Chawla	Department of Physics, Zakir Husain Delhi College, University of Delhi, New Delhi 110 002 INDIA
M. Fahim	Department of Physics, Zakir Husain Delhi College, University of Delhi, New Delhi 110 002 INDIA

ABSTRACT

A novel ferroelectric ceramic (Sr0.3Ba0.7TiO3-Sr0.3Ba0.7Nb2O6) was fabricated from powders obtained through sol-gel technique using precursors of strontium, barium and titanium. These powders were synthesized using a chemical route by in-situ gelation of Ba-Sr-Ti sol and colloidal suspension of Nb2O5 powder in butanol dissolved Titanium butoxide precursor. As-fired powder was annealed at 850oC for 3 hours in a muffle furnace. The annealed powder was cold-pressed into pellets which were then sintered at 1200oC for two hours to form dense ceramics. Structural characterization of powders was done using x-ray diffraction and Raman spectroscopy. Dielectric measurements on ceramics were done using Agilent LCR meter to study the effect of the unique combination of SBT(0.5wt%) and SBN(0.5wt%) on temperature and frequency dependent dielectric properties of bulk ceramic. It was interesting to observe that the ceramic showed significantly different dielectric behavior than that of individual Sr0.3Ba0.7TiO3(SBT) and Sr0.3Ba0.7Nb2O6 (SBN) ceramic. The results were attributed to the strong microstructural changes that occurred due to the presence of different crystalline phases.

1.0 Introduction

Strontium barium niobate ($Sr_xBa_{1-x}Nb_2O_6$) (SBN) has a tetragonal tungsten-bronze structure for $0.26<x<0.87$ and is a ferroelectric crystal at room temperature. This material possesses excellent photorefractive, electro-optic, nonlinear optic (NLO), and dielectric properties, by virtue of which they are promising material for modern day applications such as infra-red detectors, memories, phase conjugation, generation of photorefractive solitons, quasi-phase-matched second-harmonic generation, and electro-optic modulation **[1-11]**. Structural parameters as well as ferroelectricity of SBN strongly depend upon Sr/Ba molar ratio. For instance, the unit cell parameters vary almost linearly with composition, a = 12.448 to 12.412ºA and c = 3.974 to 3.905ºA for x = 0.32 to 0.82 **[12]**. Likewise, the Curie temperature (T_c) of the SBN crystals also varies with composition and is in the range of 10 to 225ºC for x = 0.82 to 0.32 respectively. These ceramics with different compositions have been produced with a high density and fairly good electrical properties using various fabrication techniques **[13-19]**. However, the dielectric, piezoelectric and pyroelectric properties of SBN ceramics exhibit smaller coefficients than those observed in single crystals, probably due to a lower degree of orientation **[16]**. The other limitations are firstly high sintering temperatures (T_s >1300ºC) and secondly very fine powders (~1 μm), often produced by ball milling, are required **[14-19]**. This results in a major increase in the cost of production and chances of contamination. In order to overcome these constraints, additives are commonly used in the fabrication of ceramics to aid in densification, control grain growth, and enhance desired properties. For instance, vanadium pentoxide V_2O_5, which melts at 690ºC, is used to accelerate the sintering and densification process. Nishiwaki et. al. **[19]** used V_2O_5 as a densification agent for SBN30 powders and reported a high dielectric constant with an addition of 1 wt% V_2O_5. Oral and Mecartney **[20]** have also studied the role of V_2O_5 as a dopant for sol-gel derived strontium barium niobate $Sr_xBa_{1-x}Nb_2O_6$ (SBN) powder and ceramics with different Sr/Ba ratios. These authors also reported that vanadium pentoxide V_2O_5 additions not only increases the densification but also the amount of tungsten bronze phase and hence the dielectric constant for all compositions except $Sr_{0.65}Ba_{0.35}Nb_2O_6$ (SBN65). For $Sr_xBa_{1-x}Nb_2O_6$ (SBN, $0.3 \leq x \leq 0.7$) ceramics, it has been reported that with increasing Sr/Ba ratio in SBN ceramics, the Curie temperature decreases while the maximum dielectric constant at the Curie temperature increases **[21]**. For x = 0.4 and 0.5 frequency dispersion of dielectric constant has been observed indicating a relaxor nature of SBN. In the recent years, the fabrication of SBN-SBT composite ceramics have generated a lot of interest **[22,23]**. For instance Shanming et.al **[24]** showed that with the addition of SBT, the maximum dielectric constant of SBN is increased and the dielectric loss is reduced. The dielectric curves become broader. The abnormal grain growth that is usually observed in $Ba_{0.6}Sr_{0.4}Nb_2O_6$ is also suppressed by the addition of $Ba_{0.6}Sr_{0.4}TiO_3$.The Curie temperature decreased with increasing amounts of BST and all samples obeyed the Curie–Weiss law above the Curie temperature. Investigations have also been reported on the fabrication of strontium barium niobate/barium strontium titanate ceramics by powder−sol method **[25]**. SBN/SBT composite ceramics with different mole ratios of Nb and Ti were fabricated using a powder sol (PS) method with Nb_2O_5 fine powders suspended in the barium strontium titanate solution. The X-ray diffraction results indicated that three intermediate phases, i.e. TiO_2, $BaNb_2O_6$ and $SrNb_2O_6$, are developed during the formation of SBN-BST. Unit-cell parameters, density, site-occupancy factors and inter-ionic distances strongly depend on the composition **[26].**

However, dielectric and pyroelectric properties of these composites have not been yet reported. Hence, in this work dielectric properties of SBN-SBT composite ceramic are being reported.

2.0 Materials and methods

2.1 Raw material and synthesis of powder and ceramic

Synthesis of SBT powder and ceramic

The starting materials were Barium acetate [$Ba(CH_3COO)_2$ ≥99%], Strontium acetate [$Sr(CH_3COO)_2$] and Titanium tetrabutoxide (97%). Acetic acid [$CH_3COOH \geq 99.7\%$] and butyl alcohol [$C_4H_9OH > 99.5\%$] were used as solvents. Calculated amounts of Barium acetate and strontium acetate were weighed to synthesize stoichiometric compositions of ($Ba_xSr_{1-x}TiO_3$) (where molar concentration x = 0.7) [(Ba+Sr):Ti = 1:1] powders. The weighed amounts of these compounds were dissolved in acetic acid by refluxing for 15 min using a heating mantle. The Ba-Sr solution was cooled down to the room temperature and the solution of calculated amount of Titanium tetrabutoxide in butanol was added and the resulting solution was stirred again using a magnetic blender for 0.5h at room temperature. After stirring, small amount of acetylacetone ($CH_3COCH_2COCH_3$) was added as stabilizer. After a few minutes the sol was hydrolysed using 10-15ml of distilled water. The sol was relatively clear and stable .The sol was covered with aluminium foil. The sol was left over-

night in open for gelation. The obtained gel was fired at 350°C in air for 3-4 hrs .The as–fired powder obtained was amorphous in nature .This powder was calcined at 850°C for 3 hrs in a muffle furnace to obtain a poly-crystaline powder. The SBT powder so obtained was milled and die-pressed into thick pellets under a pressure of 300MPa. The samples were finally sintered at 1100°C for 2h.

Synthesis of SBN powder and ceramic

The calculated amount of Niobium (V) pentoxide mixed with propan-2-ol was added in the Ba-Sr sol. The resulting solution was stirred again using a magnetic blender for 0.5h at room temperature followed by ultrasonic stirring for 10min. After this hydrolysis was done using deionized water. The sol of barium and strontium so obtained and suspended with niobium (V) pentoxide was fired at 350°C in air for 3-4 hrs .The fired powder obtained was amorphous in nature. This powder was calcined at 850°C for 3 hrs in a muffle furnace to obtain a poly-crystalline powder. The SBN powder so obtained was milled and die-pressed into thick pellets under a pressure of 300MPa

Synthesis of SBN-SBT powder and ceramic

SBT sol was prepared using the same procedure described above and was named solution A. The solution of calculated amount of Titanium tetrabutoxide and Niobium (V) pentoxide in propan-2-ol (named solution B) was added slowly drop by drop and the resulting solution was stirred again using a magnetic blender for 0.5h followed by ultrasonic stirring at room temperature. After stirring, hydrolysis was carried out using deionized water. The sol suspended with niobium (V) pentoxide was fired at 350°C in air for 3-4 hrs .The as–fired powder obtained was amorphous in nature. This powder was calcined at 850°C for 3 hrs in a muffle furnace to obtain a poly-crystalline powder. The SBN-SBT powder so obtained was milled and die-pressed into thick pellets under a pressure of 300MPa. The samples were finally sintered at 1100°C for 2h. The powder and the ceramics were prepared using a procedure given in the flow chart **(Fig. 2.1)**

2.2 Material Characterization

2.2.1 Structural Characterization

X-ray diffraction

Structural characterization of SBN, SBT and SBN-SBT powder calcined at 850°C for 3 hours was done using X-ray powder diffraction. X-ray diffractograms of SBN, SBT and SBN-SBT powders are shown in **Fig. 2.2 (a-c)**. The peaks show polycrystalline nature and confirm the formation of SBN, SBT and SBT-SBN structure.

Raman Spectroscopy

Structural characterization of SBN, SBT and SBN-SBT powder calcined at 850°C for 3 hours was done using Raman Spectroscopy and the spectrograms of SBN, BST and SBN-BST powders are shown in the **Fig. 2.3**. The peaks show polycrystalline nature and confirm the formation of SBN, SBT and SBT-SBN structure.

2.2.2 Dielectric characterization

AC frequency dependent values of parallel capacitance (Cp) and loss tangent or dissipation factor (tan δ or D) of the ceramics pellets were measured using Agilent 423B precision LCR meter. The actual thickness of samples was measured using a micrometer before electroding by application of conductive silver plate using a paint brush. Electroded samples were placed in a sample cell between two electrodes and voltage was applied. The parallel capacitance (Cp) was measured on the LCR meter. Dielectric constant was calculated using the formula:

$(\epsilon)=C/C_0$.

where, $C_O(=\epsilon_o A/d)$ is the capacitance with vacuum between parallel plates and ϵ_o=8.85x10($^{-12}$ F/m) is the permittivity of free space, A is the area of electrode sample, and d is the thickness of the sample. Dissipation factor (D or tan δ) was directly measured on the LCR meter. To calculate ac conductivity, parallel capacitance (Cp) and dissipation factor (D or tan delta) from 100 Hz up to 100 KHz was measured. $\sigma_{ac}(\omega)$ was calculated by using following expression :

$\sigma_{ac}(\omega) = 2f\epsilon_o\epsilon''=2f\epsilon_o\epsilon'\tan\delta$

where tan δ is the dissipation factor, ω = 2f is the angular frequency ϵ' is the dielectric constant (ϵ"/ ϵ' = tan δ), and ϵ" is the dielectric loss.

3.1 Results and discussion

Figure 3.1a shows the temperature and frequency dependent dielectric constant of $Sr_{0.3}Ba_{0.7}Nb_2O_6$ (SBN) ceramics. It is evident from the figure that the ceramic is ferroelectric at room temperature and a transition to paraelectric phase occurred at a temperature of 352ºC at all frequencies. It is also evident from the figure that the values of dielectric constant does not differ much at room temperature at all frequencies. However, as we increase the temperature, the values of dielectric constant increase and reach a maximum around T_c and then decrease with further increase in temperature. Around Tc, at 1 kHz, a maximum dielectric constant (ϵ'max) ~518 was obtained for this ceramic. For other higher frequencies the values decreased considerably. **Fig.3.1b** shows the temperature and frequency dependent dielectric loss of the same ceramics. Dielectric loss was found to be below 0.1 at all frequencies except for 100 Hz and 120 Hz. However, at Tc the dielectric loss was also the maximum. **Figure 3.1c** shows the ac conductivity and **Fig. 3.1d** shows the I-V characterstics of the ceramic measured using a Keithley Electrometer. **Figure 3.1e** shows the room temperature dielectric constant of the ceramic at different frequencies. Compared to SBN, the dielectric behavior of $Sr_{0.3}Ba_{0.7}TiO_3$ (SBT) ceramics was slightly different as is clear from the temperature and frequency dependent dielectric behavior of the latter shown in **Fig 3.2 a,b**. **Figure 3.2a** shows the temperature dependent dielectric constant of $Sr_{0.3}Ba_{0.7}TiO_3$ ceramics at different frequencies of 100Hz, 120 Hz, 1 kHz, 10kHz, 20kHz and 100 kHz. Since the dielectric measurements were done from room temperature (30ºC onwards), the ferroelectric-to-paraelectric phase transition temperature which generally occurs at <20ºC for this material is not visible in the figure. However, the value of dielectric constant around room temperature (and hence around T_c) was found to be ~400 at 1 kHz. At higher frequencies, the values decreased considerably at all temperatures. **Figure 3.2b** shows the temperature dependent dielectric loss of the same ceramics. Dielectric loss was found to be below 0.3 at all frequencies. However, at T_c the dielectric loss was also the maximum. **Figure 3.2c** shows the ac conductivity (σ_{ac}) of the ceramic. **Figure 3.1e** shows the room temperature dielectric constant of the ceramic at different frequencies. No frequency dispersion of dielectric constant was observed.

Figure 3.3a shows the temperature and frequency dependent dielectric constant of SBT-SBN [(0.5)SBT-(0.5)SBN] composite ceramic. This composite also showed a ferroelectric nature at room temperature. However, the transition to paraelectric temperature occurred at a much lower temperature (T_c = 295ºC) compared to SBN (T_c = 352ºC). Also, the value of dielectric constant increased to ~560 at 1 kHz. **Figure 3.3b** shows the temperature dependent dielectric loss of the same ceramics. Dielectric loss slightly increased to more than 1 at T_c. **Figure 3.3c** shows the ac conductivity of the ceramic. **Figure 3.1e** shows the room temperature dielectric constant of the ceramic at different frequencies.

Figure 3.4 shows a comparison of the temperature dependent dielectric constant of all the three ceramics at a frequency of 1

kHz. It is clear from the figure that the value of dielectric constant of SBT-SBN was higher than both SBT and SBN at T_c. Also, the T_c (<300°C) of SBT-SBN was intermediate of SBT (~30°C) and SBN (>300°C).

3.2 Conclusions

Bulk ceramics of SBT, SBN, SBT-SBN ceramics prepared using fine powders derived from sol-gel method showed that addition of SBT in SBN shifts the ferroelectric-paraelectric phase transition temperature (T_c) to a lower temperature. Also, with an addition of 0.5wt% of SBT in SBN the dielectric constant is increased at all frequencies.

Acknowledgement

Authors acknowledge the University Grants Commission (UGC), India funding for this work under the Major Project scheme. One of the authors (MC) is grateful to UGC for a Project Fellowship.

Fig. 2.1: Flow chart for the preparation of SBT-SBN powder and ceramics

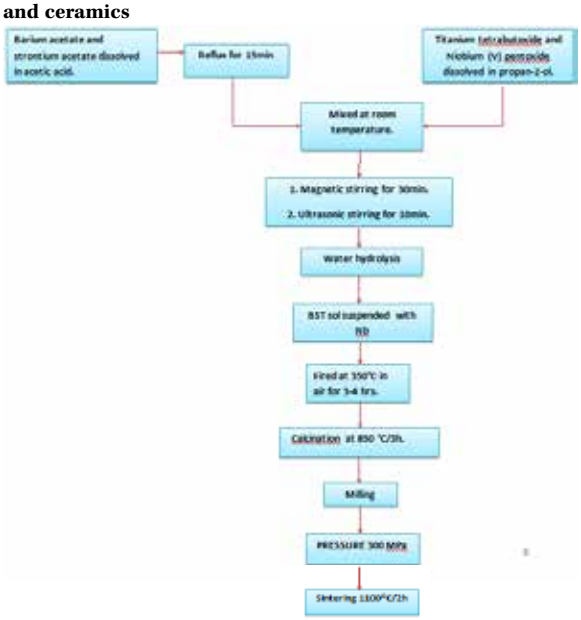

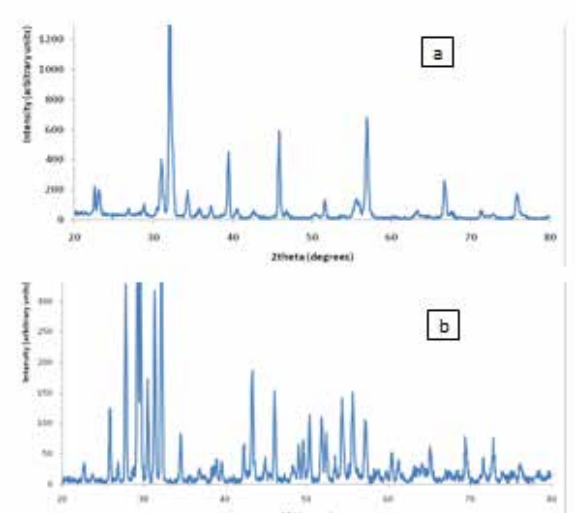

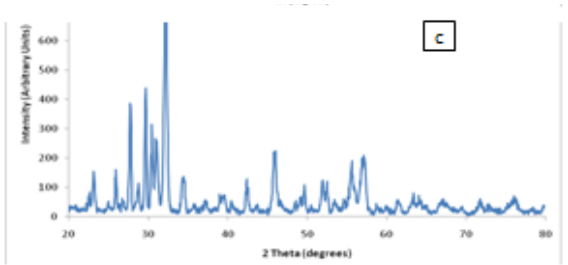

Fig. 2.2: X-ray diffractograms of (a) SBT (b) SBN (c) SBT-SBN powder

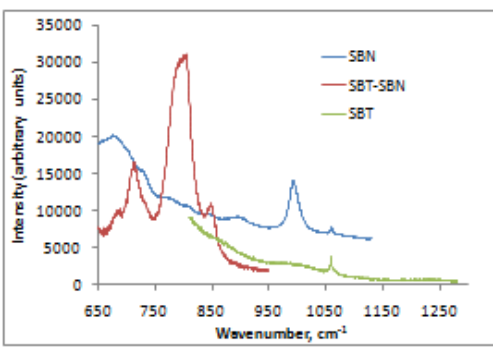

Fig. 2.3a Raman spectrographs of SBT, SBN and SBN-SBT ceramics

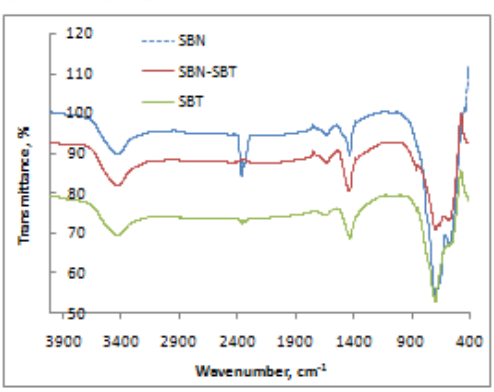

Fig. 2.3b FT-IR spectrographs of SBT, SBN and SBN-SBT ceramics

Figure 3.1: Temperature and frequency dependent dielectric properties of SBN ceramics (a) dielectric constant (b) dielectric loss (c) ac conductivity (d) I-V characteristics (e) dielectric constant at room temperature.

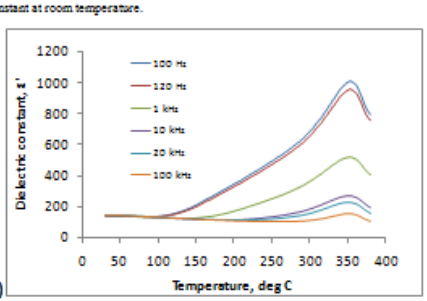

(a)

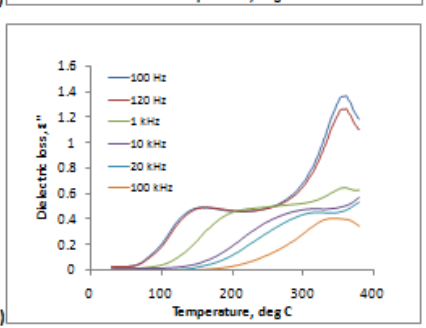

(b)

Volume : 4 | Issue : 3 | March 2015 • ISSN No 2277 - 8179

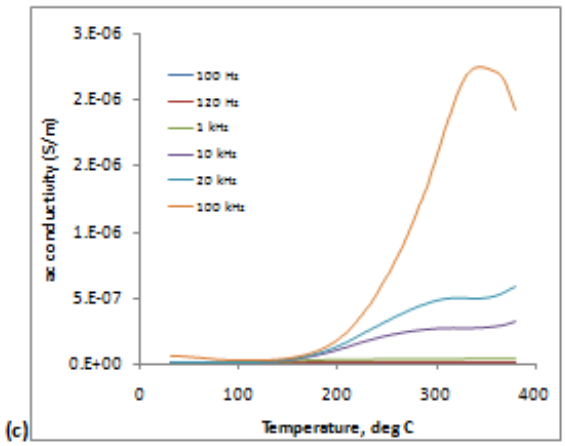

(c)

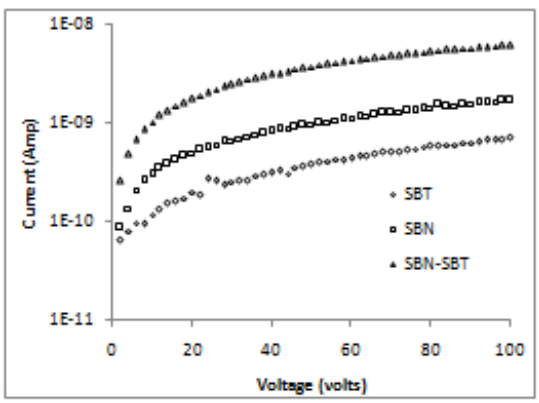

(d)

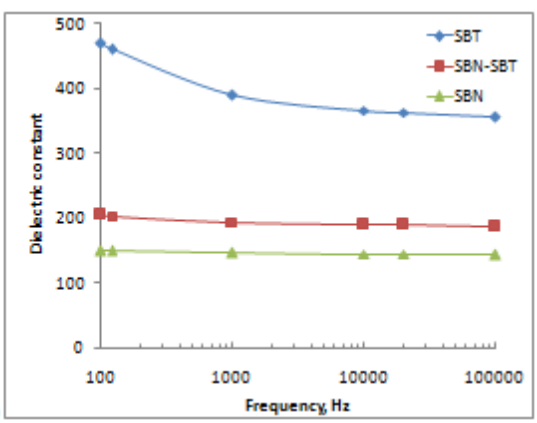

(e)

Figure 3.2: Temperature and frequency dependent dielectric properties of SBT ceramics (a) dielectric constant (b) dielectric loss (c) ac conductivity

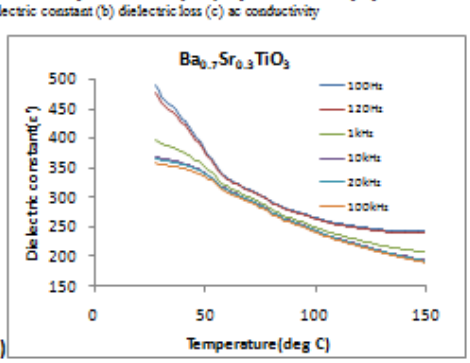

(a)

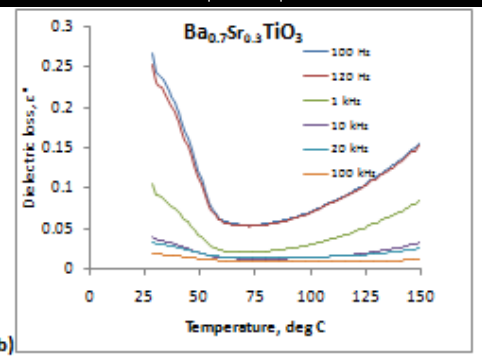

(b)

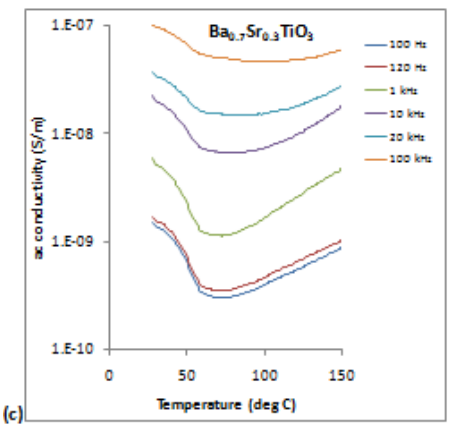

(c)

Figure 3.3: Temperature and frequency dependent dielectric properties of SBT-SBN ceramics (a) dielectric constant (b) dielectric loss (c) ac conductivity

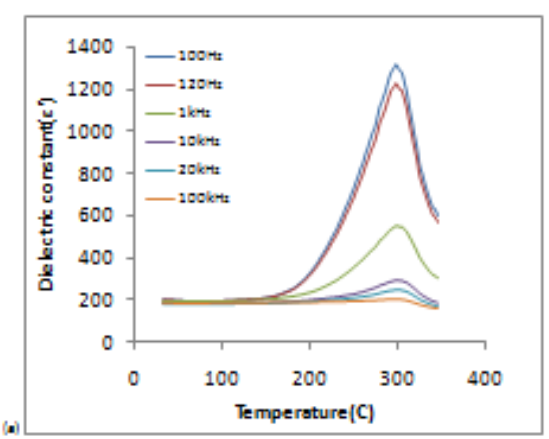

(a)

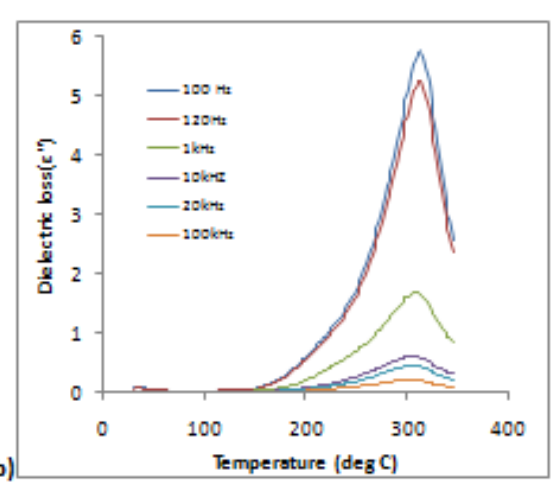

(b)

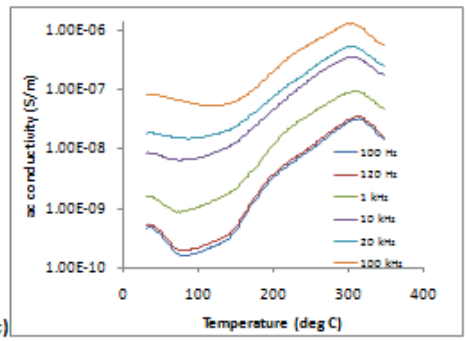

(c)

Fig. 3.4: Comparison of dielectric constant of SBT, SBN and SBT-SBN ceramics measured at 1 kHz

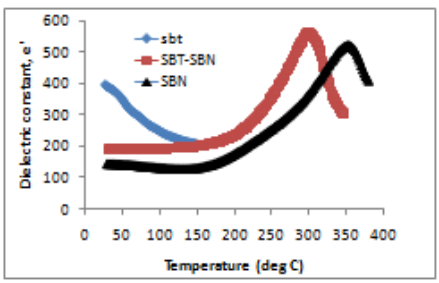

REFERENCE

[1] A. A. Ballman and H. Brown, The growth and properties of strontium barium metaniobate, Sr1-xBaxNb2O6, a tungsten bronze ferroelectric. Journal of Crystal Growth, 1, (1967) 311 | [2] M. R. Kruer, L. Esterowitz, F. J. Bartoli, and R. E. Allen, Optical radiation damage of SBN materials and pyroelectric detectors at 10.6 ^{1}m, Journal of Applied Physics, 46, (1975) 1074 | [3] A. M. Glass, Investigation of the electrical properties of Sr1-xBaxNb2O6 with special reference to pyroelectric detection, Journal of Applied Physics, 40, (1969) 4699 | [4] J. B. Thaxter, Electric control of holographic storage in strontium-barium-niobate. Applied Physics Letters, 15, (1969) 210 | [5] J. B. Thaxter and M. Kestigian, Unique properties of SBN and their use in a layered optical memory, Applied Optics, 13, (1974) 913 | [6] F. Micheron, C. Mayeux, and J. C. Trotier, Electrical control in photoferroelectric materials for optical storage, Applied Optics, 13, (1974) 784 | [7] S. Redfield and L. Hesselink, Enhanced nondestructive holographic readout in strontium barium niobate, Optical Letter, 13, (1988) 880 | [8] H. Y. Zhang, X. H. He, Y. H. Shih, and L. Yan, Picosecond phase conjugation and two-wave coupling in strontium barium niobate, Journal of Modern Optics, 41, (1994) 669 | [9] M. Wesner, C. Herden, R. Pankrath, D. Kip, and P. Moretti, Temporal development of photorefractive solitons up to telecommunication wavelengths in SBN, Physical Review E, 64, (2001) 36613 | [10] A. S. Kewitsch1, M. Segev, A. Yariv, G. J. Salam, T. W. Towe, E. J. Sharp, and R. R.Neurgaonkar, Tunable quasi-phase matching using dynamic ferroelectric domain gratings induced by photorefractive space-charge fields, Applied Physics Letters, 64, (1994) 3068 | [12] M. Ulex. ZÄuchtung und Charakterisierung von Sr1-xBaxNb2O6-Kristallen im Bereichvon 0; 32 < x < 0; 82. UniversitÄat OsnabrÄuck, Dissertation, (2004). | [13] T. Fang and N. Wu, J. Mat Sci, 30 (1995) 3376 | [14] W. Lee and T. Fang, J. Am Ceram. Soc, 81 (1998) 1019 | [15] N. Vandamme, A Sutherland, I Jones and S. Winzer, J. Am. Ceram Soc., 74 (1991) 1785 | [16] D. Spinola, E. Moriera, L. Bassora and D. Garcia, Proc. Of IEEE Ultrasonic Symp, San Antonio, Texas, Nov. 1996, Ed M. Levy, S.C. Schneider and B.R. Mcavoy (New York 1996) 523 | [17] S. Deshpande, H. Potdar and P. Godbole and S. Date, J. Am Ceram Soc., 75 (1992) 2581 | [18] W. Lee and T. Fang, ibid, 81 (1998) 300 | [19] S. Nishiwaki, J. Takahashi and K.Kodaira, Jap. J. Ap. Phys, 33 (1994) 5477 | [20] A.Y. Oral and M.L. Mecartney, J. Mat. Sci., 36 (2001) 5519 | [21] Myoung-Sup KIM, Peng WANG, Joon-Hyung LEE, Jeong-Joo KIM, Hee Young LEE and Sang-Hee CHO, Jpn. J. Appl. Phys., 41 (2002) 7042 | [22] Zhou Z H, Du P Y, Weng W J, Mater Chem and Phys, (2004), 87(2/3), 430 | [23] Niu X K, Zhang J L, Wang J F, Li C Y, Lv Y G, Electr Components and Mater, 26(4), (2007), 8 | [24] Shanming Ke, Haitao Huang, Huiqing Fan, H L W Chan and L M Zhou, J. Phys. D: Appl. Phys, 40 (2007) 6797 | [25] SHAN Lianwei, WANG Fengchun, WANG Jihua, WU Ze, HAN Zhidong, DONG Limin, ZHANG Xianyou, Trans. Nonferrous Met. Soc. China, 22 (2012) 138 | [26] Sergey Podlozhenov, Heribert A. Graetsch, Julius Schneider, Michael Ulex, Manfred Wohlecke and Klaus Betzler, Acta Cryst. B62, (2006), 960 |